Supplementary information for

Innovating Carbon-Based Perovskite Solar Cells: The Role of a CN-Anchoring Self-Assembled Molecular Layer in Efficiency and Stability

Sheida Rezakhani,[a] Hashem Shahroosvand[a] Peng Gao,[b] Mohammad Khaja Nazeeruddin[c]**

Experimental Section

Materials:

Methylammonium iodide (99%), LiTFSI (99.95%) and acetonitrile (99.8%), Graphite, $NaBH_4$ were purchased from Sigma-Aldrich. HCl (37%), PbI_2 (98%), spiro-OMeTAD, dimethylformamide (99.8%), dimethyl sulfoxide (99.9%), 2-propanol (99.5%), chlorobenzene (99.9%), ethanol (99%), polymethyl methacrylate were purchased from Merck. Graphene oxide (99%, Us Nano), carbon black (Top Nano Technology, Taiwan), TiO_2 paste (PST-20T, Sharif Solar Co., Iran), 4-tert-butyl pyridine (96%, Acros Organics) were used as received.

Characterization instruments:

-^{1}H NMR spectra were recorded on Bruker Advance 250 MHz spectrometers, locked on deuterated solvents. Chemical shifts were calibrated against tetramethylsilane as an internal standard.

-Ultraviolet-visible (UV-vis) absorption spectra of the films were obtained with Beijing Rayleigh Analytical Instrument Corp, UV-1800 spectrophotometer.

-Cyclic voltammetry (CV) measurements were examined on a SAMA500 potentiostat electrochemical analyzer with a three-electrode cell system. A glassy carbon electrode was used as the working electrode and a Pt wire was used as the counter electrode. For reference electrode, a KCl-saturated Ag/AgCl electrode was used (calibrated by Fc/Fc+ as an external reference). The -CV measurements were performed in chloroform solvent, using 0.1 M tetrabutylammonium perchlorate (TBAP) as the supporting electrolyte. - X-ray photoelectron spectroscopy (XPS) measurements were carried out on a photoelectron spectrometer (AXISULTRA DLD-600W, Kratos, Shimadzu, Japan).

- Electron microscopy (SEM) measurements and energy-dispersive analysis of the X-rays (EDAX) were performed using a MIRA3 TESCAN-XMU microscope.

-Steady-state photoluminescence (PL) spectra were recorded with an AVANTESAvaSpec-128 spectrophotometer.

-Atomic force microscopy (AFM) measurements were performed with an ARA RESEARCH microscope operating in a non-contact mode.

-The current density vs. voltage (J–V) curves were measured using a source meter SAMA500 (Newport, Oriel Class A, 91195A) under simulated 100 mA cm^{-2} illumination (AM 1.5G) and a calibrated Si reference cell certified by the National Renewable Energy Laboratory (NREL) with a KG-5 filter. A 0.100 cm^2 sized metal aperture was also used on to the device to precisely define the active area during the measurements (device active area: 0.13 cm^2). The voltage scan rate was 0.1 Vs^{-1}. The voltage window was from -0.1 V to 1.2 V.

-Incident photon-to-current conversion efficiencies (IPCE) were measured with an IPCE-020 IROSOL instrument.

-The stability of our C-PSCs is preliminarily evaluated through thermal aging and shelf-life aging (ISOS-D-1), showing satisfactory performance even without encapsulation.

-Electrochemical impedance spectroscopy (EIS) measurements were carried out using a potentiostat/galvanostat Origalys Origa Flex in the frequency range from 1 MHz to 1 Hz.

-PL quenching efficiency was calculated using the following formula:

$$\eta_{quench} = \frac{PL_{perovskite} - PL_{HSM}}{PL_{perovskite}}$$

where $PL_{perovskite}$ and PL_{HSM} are the integrated PL intensities of perovskite on glass substrates without and with the quenching HSM layer.

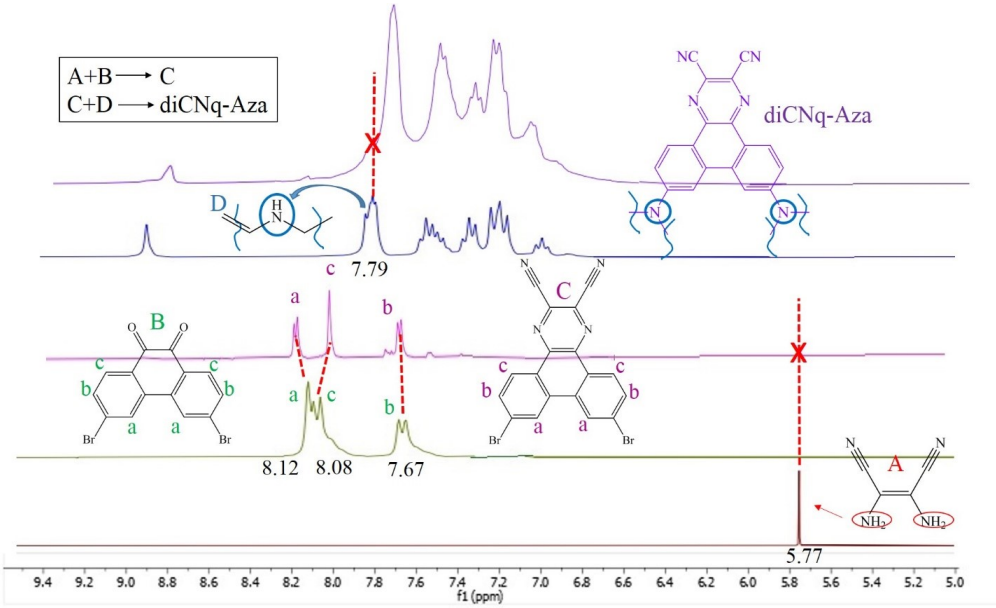

Figure S1. [1]H-NMR spectra of the materials. The red, green, pink, blue and purpel spectra correspond to the materials 2,3-diaminomaleonitrile (A), 3,6-dibromophenanthrene-9,10-dione (B), 7,10-dibromo benzo [f.h] quinoxaline-2,3-dicarbonitrile (C), 4-phenylazo diphenylamine (D) and diCNq-Aza, respectively.

Comment [r]: Following the comments of referee 2, the [1]H-NMR and FTIR spectra were included in the supplementary (Figs. S1 and S2).

Referee 2

4. The molecular structures of diCNq-Aza and spiro-OMeTAD should be characterized via NMR, FTIR, etc.

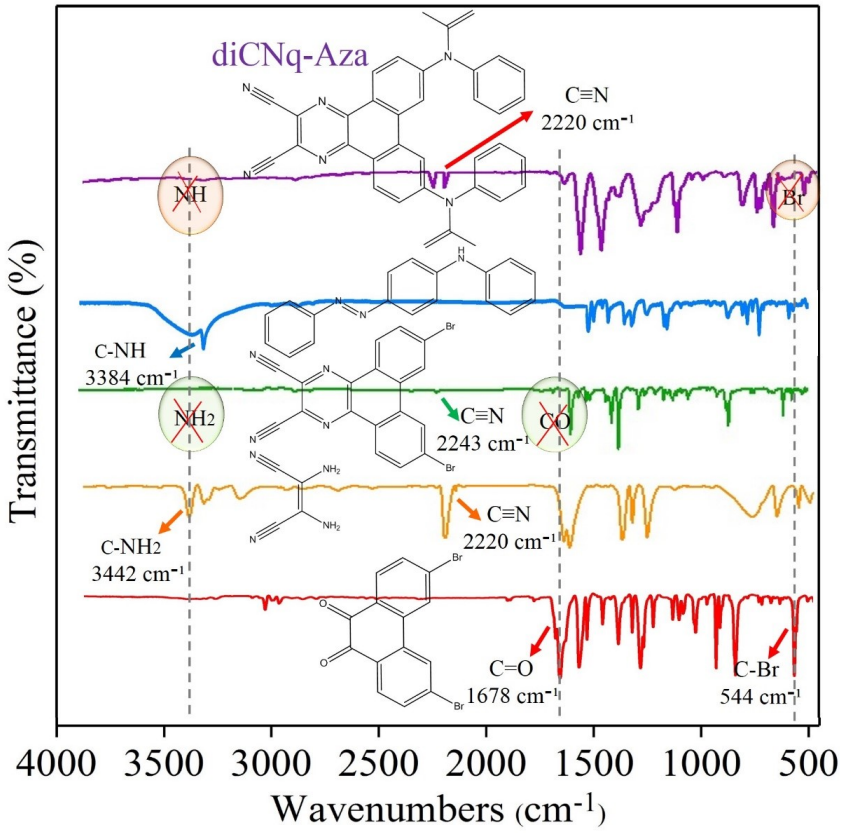

Figure S2. FTIR spectra of the materials. The red, yello, green, blue and purpel spectra correspond to the materials 3,6-dibromophenanthrene-9,10-dione, 2,3-diaminomaleonitrile, 7,10-dibromo benzo [f.h] quinoxaline-2,3-dicarbonitrile, 4-phenylazo diphenylamine and diCNq-Aza, respectively.

Comment [r]: Following the comments of referee 2, the ^{1}H-NMR and FTIR spectra were included in the supplementary (Figs. S1 and S2).

Referee 2

4. The molecular structures of diCNq-Aza and spiro-OMeTAD should be characterized via NMR, FTIR, etc.

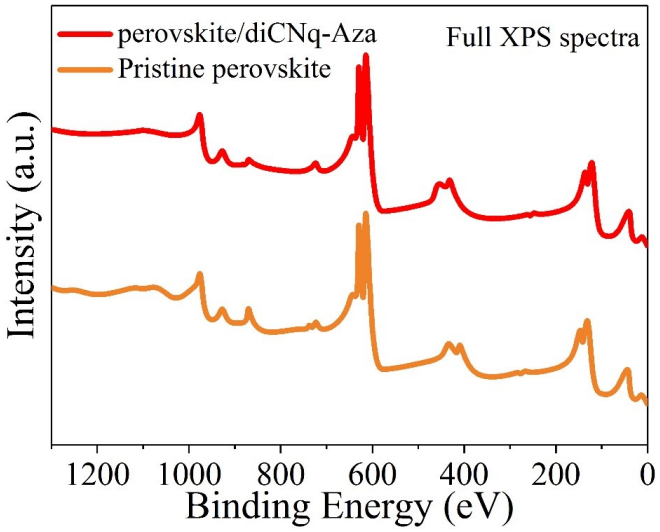

Figure S3. Full survey XPS spectra of perovskite films with and without diCNq-Aza passivation treatment.

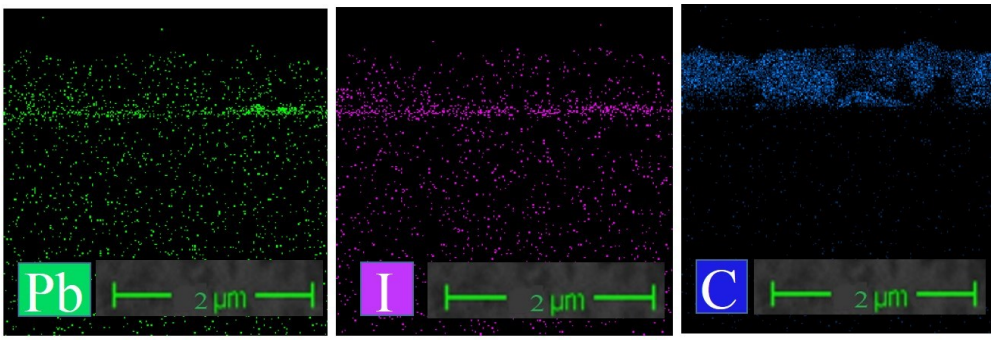

Comment [r]: In response to the second comment of reviewer 3, XPS and FTIR spectra for p/diCNq-Aza were recorded, analyzed and reviewed to investigate the interaction between the new HSM and the perovskite.

Referee 3

2. The claim that the SAM penetrates into the perovskite and passivates bulk traps based on EDX data is not fully convincing. Supporting evidence such as XPS measurements would strengthen this conclusion.

Figure S4. EDX map for Pb, I and C atoms.

Comment [r]: We changed the EDX mapping in Figure 3c and fore more details we added new EDX map in Figure S4.

Referee 2
1.The EDX mapping is not clear.

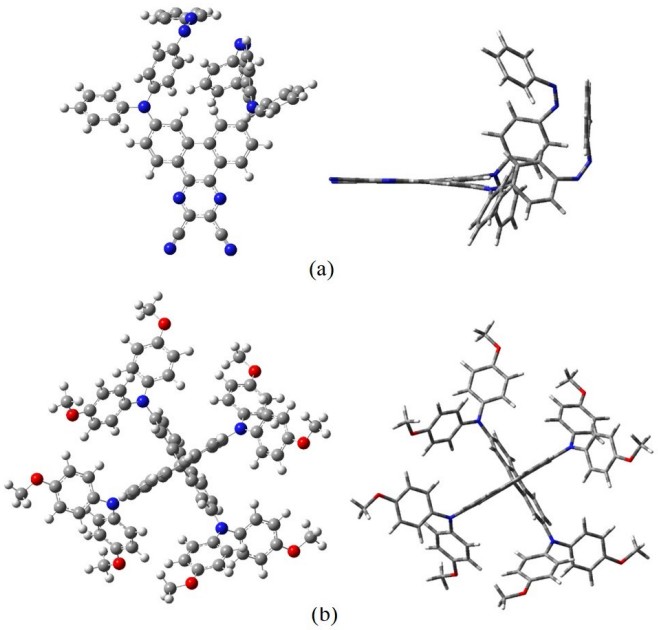

Figure S5. Top view (left) and Side view (right) of optimized geometry of diCNq-Aza; **(a)** and spiro-OMeTAD **(b).**

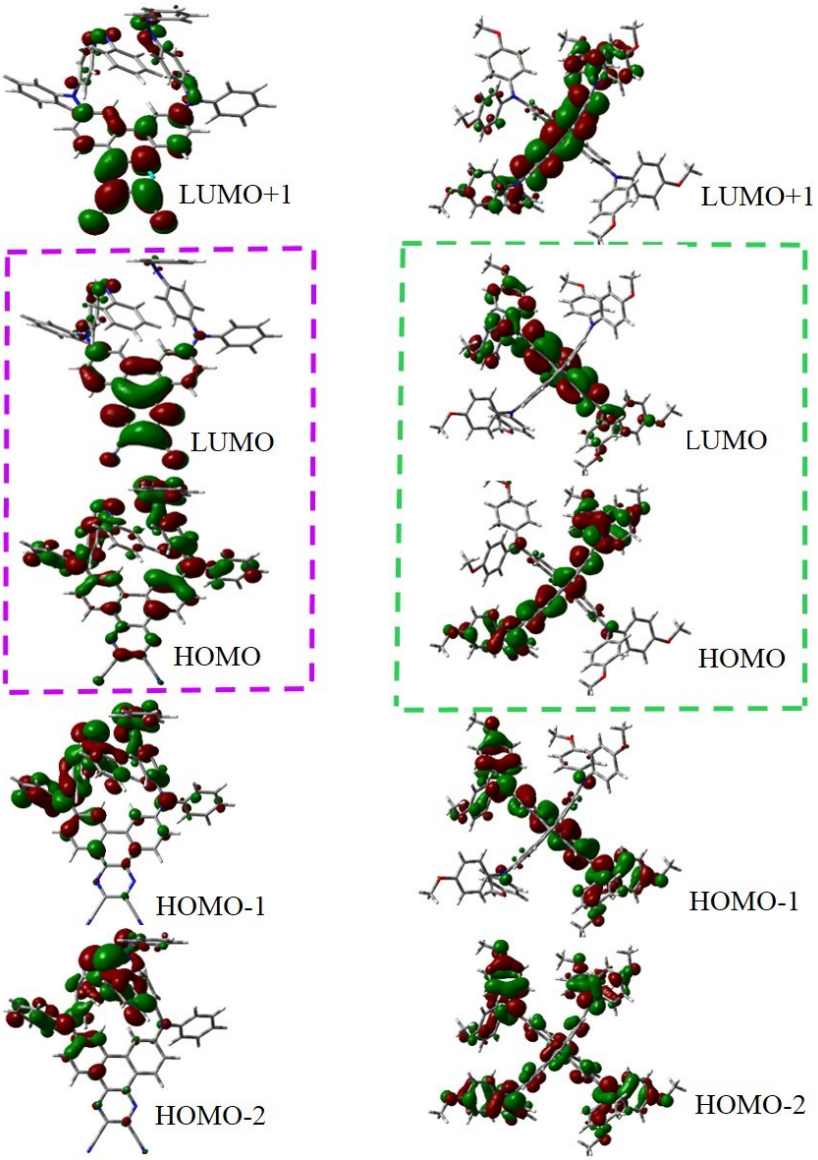

Figure S6. DFT calculated frontier molecular orbitals of LUMO+1, LUMO, HOMO, HOMO-1 and HOMO-2 energy levels of diCNq-Aza (left) and spiro-OMeTAD (right).

Comment [r]: We removed that the HOMO/LUMO values from DFT calculation for more accuracy.

Referee 3

1. *The discrepancy between the HOMO/LUMO values measured by CV and DFT requires further explanation.*

Hole transfer rate (K_h)

Einstein-Smolochovsky equation was used to calculate the hole mobility (μ) of the HSMs, and Km which is related to hopping rate (the same K_h) is obtained from the Marcus theory:

$$K_h = \frac{4\pi^2}{h} V^2 \frac{1}{\sqrt{4\pi\lambda_h K_B T}} exp\left[-\frac{\lambda_h}{4K_B T} \right]$$

where h, K_B, T and λ_h are the Planck's constant, the Boltzmann's constant, the room temperature (T = 300 K) and the hole reorganization energy, respectively. The hole reorganization energy (λ_h) is defined by:

$$\lambda_h = \left(E^{+}_{0} - E_{+} \right) + \left(E^{0}_{+} - E_0 \right)$$

where E^{+}_{0} and E_{+} represent the cationic energy of the neutral optimized molecule and the cationic energy based on the optimized cationic structure, respectively; E^{0}_{+} is the neutral molecular energy based on optimized cationic molecule; and E_0 is the energy of the structure of the optimal neutral molecule. V_h denotes hole transfer integral, which can be calculated from the following formula:

$$V_h = \frac{E_{HOMO} - E_{HOMO-1}}{2}$$

In order to create a good coating of HSM film on the perovskite film in PSCs, HSM must be strongly soluble in the solvent (e.g., chlorobenzene), and for this purpose, the solubility of HSM can be calculated using solvation free energy (ΔG_{sol}). It is defined as the difference between the free energy of the molecule in the gas phase and free energy of the molecule in the solution phase. In this work, we have calculated the solubility of the diCNq-Aza in two different solvents: (i)

DMSO and (ii) dichloromethane (DCM). Further, the calculated results indicated that the diCNq-Aza has better solubility in DMSO in comparison to DCM (see Table S1). The better solubility of the diCNq-Aza will facilitate easy fabrication of the efficient PSCs.

Solubility and Stability

In order to create a good coating of HSM film on the perovskite film in PSCs, HSM must be strongly soluble in the solvent, and for this purpose, the solubility of HSM can be calculated using solvation free energy (ΔG_{solv}). It is defined as the difference between the free energy of the molecule in the gas phase and free energy of the molecule in the solution phase. In this work, we have calculated the solubility of HSMs in chlorobenzene (PhCl). Results of Table S1indicated that the values of ΔG_{solv} for both HSMs are negative and favorable.

The stability of the diCNq-Aza molecule is checked by calculating its chemical hardness value (η), which is obtained from the relation $(E_{HOMO} - E_{LUMO})/2$. The large value of η corresponds to higher stability of the HSMs. In this work the value of η indicate that the stability of the diCNq-Aza is comparable to that of spiro-OMeTAD. Further, in order to use the diCNq-Aza as a passivation layer on the perovskites, we have also calculated its dipole moment, that is found to be nearly close to zero, it shows the hydrophobic nature of this molecule. All calculated results are listed in Table S1.

Table S1. The Calculated Values of Solubility in chlorobenzene, Chemical Hardness, Dipole Moment of diCNq-Aza and spiro-OMeTAD

Molecules	ΔG_{solv} (eV)	η (eV)	dipole moment (Debye)
diCNq-Aza	-0.65	1.35	6.426
spiro-OMeTAD	-16.43*	1.81	5.965

* From Solar Energy 173 (2018) 132-138

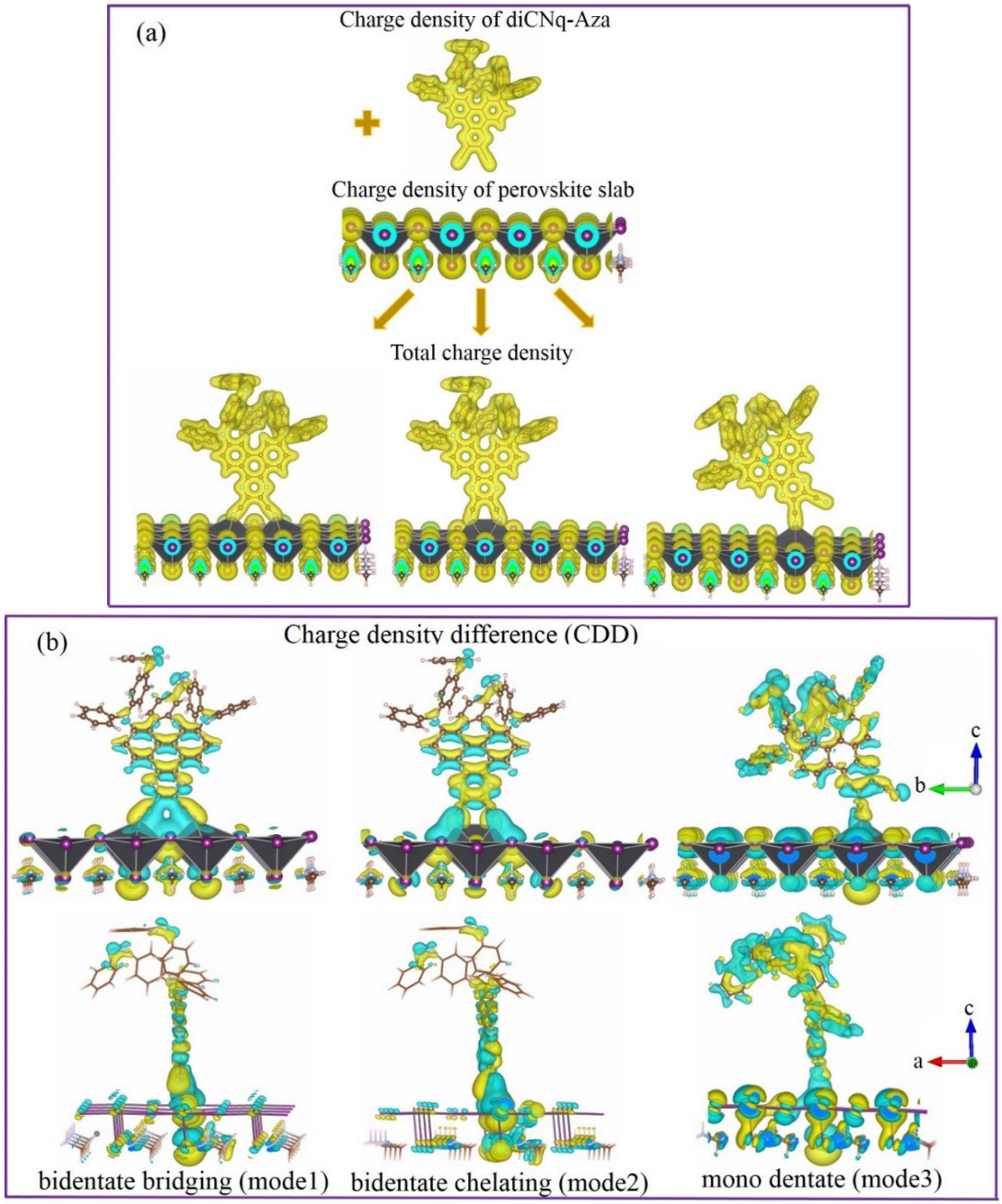

Figure S7. (a) Charge density distribution of diCNq-Aza and perovskite slab. (b) Charge density differences for optimized structure of the adsorbed diCNq-Aza /perovskite system in three different modes, calculated using the VASP code. Charge accumulation is shown in yellow while charge depletion is in blue.

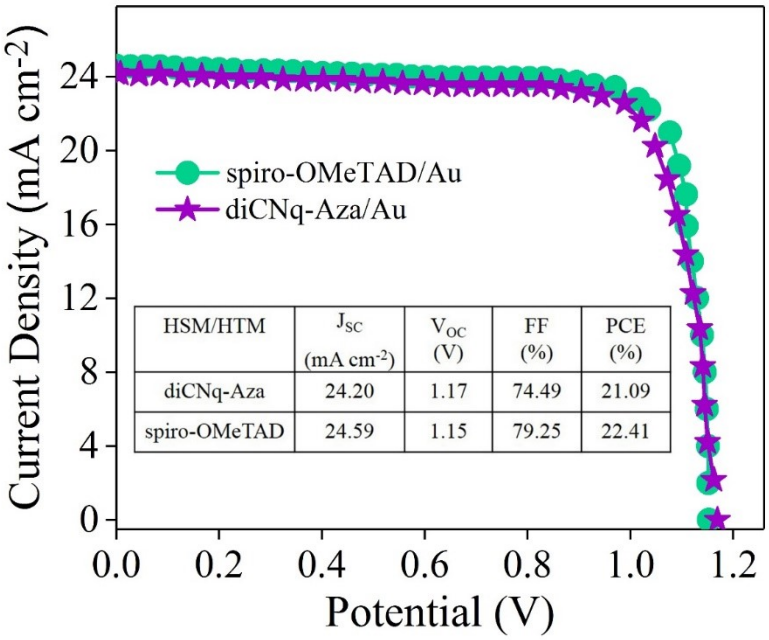

Figure S8. J–V curves of the PSCs based on Au electrode with diCNq-Aza and spiro-OMeTAD as HSM/HTM.

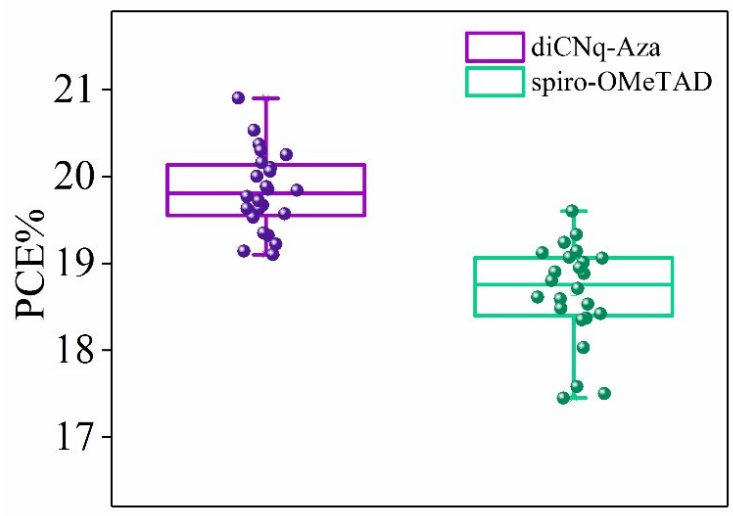

Figure S9. Statistical analysis of PCE for 24 devices of diCNq-Aza and spiro-OMeTAD based PSCs (FTO/TiO_2/$MAPbI_3$/HSM/C).

Table S2. The obtained photocurrent decay times ($\tau_{transport}$) and photovoltage decay times ($\tau_{recombination}$) of perovskite solar cells based on diCNq-Aza and spiro-OMeTAD.

HSM/HTM	$\tau_{transport}$ (μs)	$\tau_{recombination}$ (μs)
diCNq-Aza	3.28	11.89
spiro-OMeTAD	7.21	5.36

Table S3. The detailed data of the Nyquist plot of diCNa-Aza and spiro-OMeTAD based devices

HSM/HTM	Rs (Ω)	Rrec (Ω)	Crec (nF)
diCNq-Aza	21.59	530.8	5.212
spiro-OMeTAD	81.96	404.6	7.298

Table S4. Summary of certified photovoltaic parameters of PSCs using SAM HSM/HTMs published in recently eight years

HSM/HTM	Device structure	J_{sc} mAcm^{-2}	V_{oc} (V)	FF (%)	PCE (%)	Year	Refs
diCNq-Aza	FTO/TiO_2/$MAPbI_3$/diCNq-Aza/C	22.27	1.18	75.58	20.37	2024	Our work
MPA-BT-CA	ITO/MPA-BT-CA/perovskite/C_{60}/ZrAcac/Ag	23.12	1.13	80.90	21.21	2022	1
BTORCNA	ITO/BTORCNA/perovskite/C_{60}/BCP/Ag	22.84	1.10	84.00	21.10	2022	2
D33	ITO/D33/$MAPbI_3$/$PC_{61}BM$/BCP/Ag	22.19	1.02	78.80	17.85	2020	3
ICTH1	FTO/Meso-TiO2/$MAPbI_3$/ICTH1/Ag	24.56	1.01	72.20	17.91	2018	4
ICTH2	FTO/Meso-TiO2/$MAPbI_3$/ICTH2/Ag	24.78	1.03	73.50	18.75	2018	4
KR321	ITO/$(FAPbI_3)0.85(MAPbBr_3)0.15$/PEDOT:PSS/KR321/Au	21.70	1.13	78.00	19.03	2017	5

Comment [r]: *TPC and TPV analyses for the new HSM and spiro-OMeTAD*

Referee 3
4. Including TPC measurements would provide more direct insight into improvements in charge extraction.

Comment [r]: The results of photocurrent and electrochemical impedance spectroscopy measurements are indicated in green highlights. The graphs and relevant data are shown in Figure 6a, Table 3, and Figure 6e, Table S3, respectively.

Referee 2
2. Please provide both photocurrent measurements and electrochemical impedance spectroscopy (EIS) results.

KR353	ITO/$(FAPbI_3)0.85(MAPbBr_3)0.15$/PEDOT:PSS/KR353/Au	19.31	1.11	69.00	14.87	2017	5	
KR355	ITO/$(FAPbI_3)0.85(MAPbBr_3)0.15$/PEDOT:PSS/KR355/Au	16.01	1.05	53.00	8.88	2017	5	
MPA-Ph-CA	ITO/MPA-Ph-CA/$Cs_{0.05}(FA_{0.92}MA_{0.08})_{0.95}Pb(I_{0.92}Br_{0.08})_3$/$C_{60}$/Ag	23.62	1.13	82.48	22.05	2024	6	
FMPA-BT-CA	ITO/FMPA-BT-CA /$(FA_{0.17}MA_{0.94}PbI_{3.11})_{0.95}$ $(PbCl_2)_{0.05}$/C_{60}/BCP/Cu	23.33	1.15	83.30	22.37	2022	7	
2FMPA-BT-CA	ITO/2FMPA-BT-CA /$(FA_{0.17}MA_{0.94}PbI_{3.11})_{0.95}(PbCl_2)_{0.05}$/$C_{60}$/BCP/Cu	22.81	1.14	83.10	21.68	2022	7	
Cz-CA	ITO/Cz-CA/$Cs_{0.05}(FA_{0.92}MA_{0.08})_{0.95}Pb(I_{0.92}Br_{0.08})_3$/PCBM C_{60}/Ag	23.20	1.06	83.00	20.00	2022	8	
TPA-CA	ITO/TPA-CA/$Cs_{0.05}(FA_{0.92}MA_{0.08})_{0.95}Pb(I_{0.92}Br_{0.08})_3$/PCBM C_{60}/Ag	22.40	1.06	81.00	17.50	2022	8	
MPA-CA	ITO/MPA-CA/$Cs_{0.05}(FA_{0.92}MA_{0.08})_{0.95}Pb(I_{0.92}Br_{0.08})_3$/PCBM C_{60}/Ag	23.50	1.10	81.00	20.50	2022	8	
Cz-Ph-CA	ITO/Cz-Ph-CA/$Cs_{0.05}(FA_{0.92}MA_{0.08})_{0.95}Pb(I_{0.92}Br_{0.08})_3$/PCBM C_{60}/Ag	23.00	1.11	83.00	20.20	2022	8	
TPA-Ph-CA	ITO/TPAPhCA/$Cs_{0.05}(FA_{0.92}MA_{0.08})_{0.95}Pb(I_{0.92}Br_{0.08})_3$/PCBM C_{60}/Ag	23.00	1.12	82.50	20.00	2022	8	
PQxD	ITO/PQxD/$FASnI_3$/C_{60}/BCP/Ag	19.28	0.54	68.10	7.10	2023	9	
TQxD	ITO/PQxD/$FASnI_3$/C_{60}/BCP/Ag	21.05	0.57	68.80	8.30	2023	9	

Figure S10. Molecular structures of SAML HTMs with cyanoacetic acid (CAA) anchoring groups.

Table S5. Statistical stability data of J_{sc}, V_{oc}, FF and PCE for the PSCs (FTO/TiO_2/$MAPbI_3$/HSM/C) based on diCNq-Aza.

HSM	Time (h)	J_{sc} (mA/cm^2)	V_{oc} (V)	FF	PCE (%)
diCNq-Aza	0	22.27	1.160	78.85	20.37
	50	21.78	1.170	83.25	20.61
	100	22.25	1.165	75.43	19.54
	150	22.31	1.162	73.88	19.16
	200	21.97	1.191	71.06	18.56
	250	21.75	1.178	72.08	18.45
	300	22.24	1.160	73.02	18.83
	350	22.29	1.165	74.40	19.32
	400	21.86	1.169	75.21	19.22
	450	21.67	1.171	75.19	19.08
	500	21.32	1.159	77.18	19.07
	550	21.80	1.172	74.59	19.06
	600	21.51	1.155	76.53	19.01

Table S6. Statistical thermal stability data of J_{sc}, V_{oc}, FF and PCE for the PSCs (FTO/TiO_2/$MAPbI_3$/HSM/C) based on diCNq-Aza in 80°C.

HSM	Time (h)	J_{sc} (mA/cm^2)	V_{oc} (V)	FF	PCE (%)
diCNq-Aza	0	22.11	1.160	73.33	19.62
	50	22.13	1.170	76.64	20.02
	100	22.37	1.162	80.15	20.82
	150	22.40	1.180	75.29	19.90
	200	22.18	1.166	74.59	19.29
	250	22.04	1.175	74.83	19.38
	300	21.58	1.161	77.51	19.42
	350	22.08	1.174	74.99	19.44
	400	21.58	1.168	77.25	19.47
	450	22.02	1.160	76.50	19.54
	500	22.12	1.181	74.26	19.40
	550	21.90	1.177	74.60	19.23
	600	21.97	1.165	74.70	19.12

Table S7. The thermal stability of PSCs based on different HSM/HTMs from past literature.

HSM/HTM	Temperature (°C)	Initial PCE (%)	PCE maintenance rate % (Time)	Refs
diCNq-Aza	80	19.62	97.45 (600 h)	Our work
spiro-OMeTAD	85	13.40	54.14 (250 h)	10
TQ4	85	20.5	90 (110 h)	11
PE10	85	22.3	80 (500 h)	12
PC3	85	20.8	80 (200 h)	13
DTB-FL	80	21.5	68 (240 h)	14
XF2	85	19.17	80 (768 h)	15
XF3	85	20.59	80 (768 h)	15
P3HT	80	20.5	91.11(500 h)	16
PTAA	80	22.8	78.52 (500 h)	16
ZT-H2	60	19.63	90 (408 h)	17
DBTMT	65	21.1	65 (54 h)	18
DFBT–PMTP	65	21.2	60 (145 h)	19
DFBT–MTP	65	20.1	80 (280 h)	20
BT–MTP	65	14.9	80 (280 h)	20

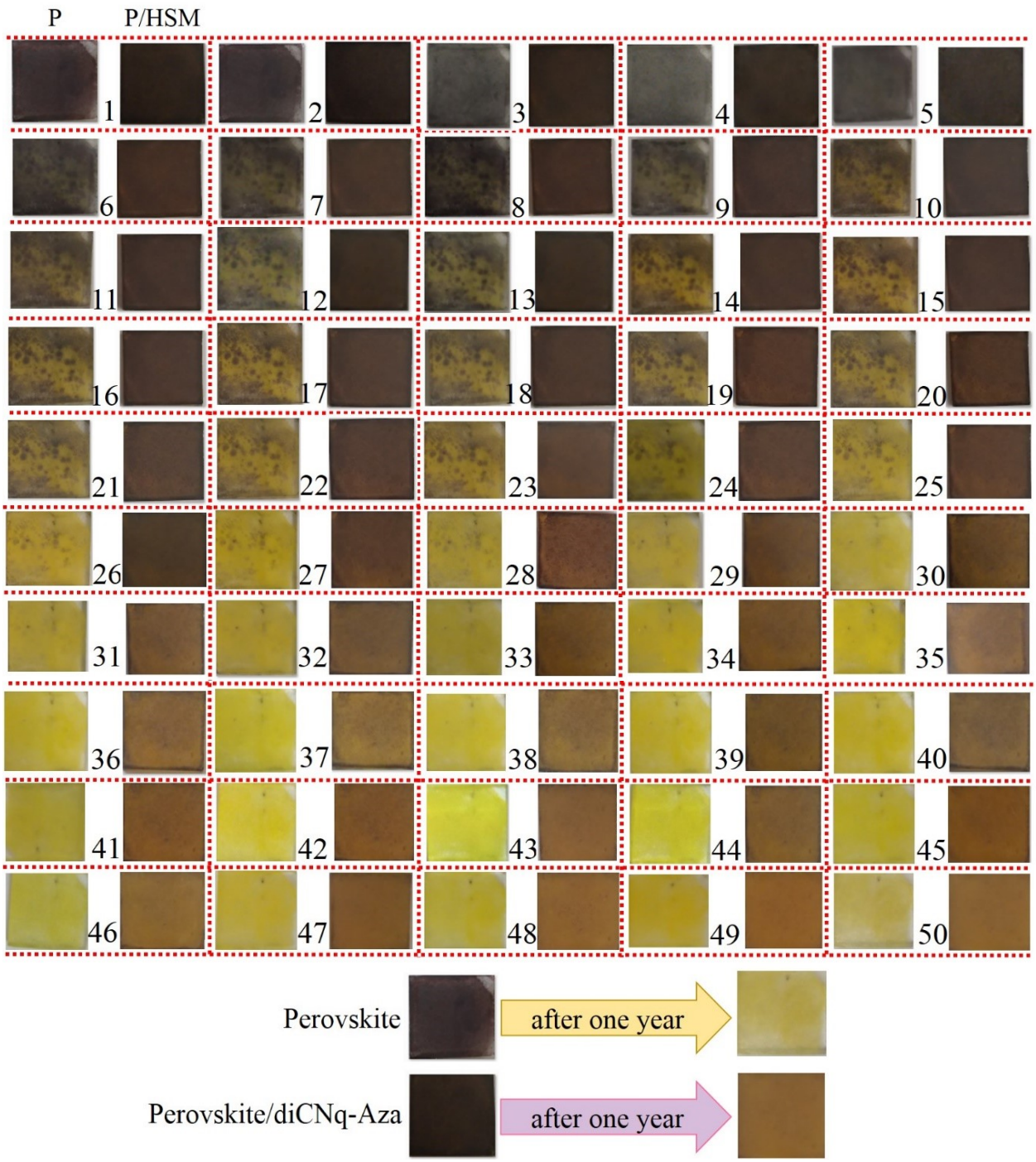

Figure S11. The photo-stability of perovskite films and films of the new SAM-HSM coated on perovskite layer for one year by photographic images (this report is week by week and numbers in the figure correspond to the number of weeks). In each pair of separate images, the left image is the perovskite film and the right image is the P/diCNq-Aza film.

Table S8. The cost of materials that used to synthesis 1 gram of diCNq-Aza.

	Chemical	Weight (g)	Price ($/g)	Price of used chemical ($)	Cost per step ($/step)
Step 1	3,6-dibromophenanthrene-9,10-dione	0.58	6.90	4.00	4.460
	2,3-diaminomaleonitrile	0.17	0.37	0.06	
	Acetic acid	10.0	0.04	0.40	
Step 2	4-phenylazo diphenylamine	0.78	25.81	20.13	23.056
	CuI	0.05	1.46	0.073	
	1,10-phenanthroline	0.10	2.93	0.293	
	Cs_2CO_3	2.00	1.08	2.160	
	DMF	5.00	0.08	0.400	
	Total				27.516

Comment [r]: Estimate the cost of producing the new synthetic molecule and compare it with values reported for spiro-OMeTAD and several other HTMs in previous studies. (Figure 8, Table S8).

Referee 2

3. Provide a short cost-benefit analysis table or figure to visually compare this work vs. other electrodes in terms of materials and performance.

References

1 Q. Liao, Y. Wang, Z. Zhang, K.Yang, Y. Shi, K. Feng, B. Li, J. Huang, P. Gao and X. Guo, *Journal of Energy Chemistry*, 2022, **68**, 87-95.

2 K. Yang, Q. Liao, J. Huang, Z. Zhang, M. Su, Z. Chen, Z. Wu, D. Wang, Z. Lai and H. Y. Woo, *Angewandte Chemie International Edition*, 2022, **61** (2), e202113749.

3 L. Duan, Y. Chen, J. Yuan, X. Zong, Z. Sun, Q. Wu and S. Xue, *Dyes and Pigments*, 2020, **178**, 108334.

4 D. Bharath, M. Sasikumar, N. R. Chereddy, , J. R. Vaidya and S. Pola, *Solar Energy*, 2018, **174**, 130-138.

5 K. Rakstys, S. Paek, P. Gao, P. Gratia, T. Marszalek, G. Grancini, K. T. Cho, K. Genevicius, V. Jankauskas and W. Pisula, *Journal of Materials Chemistry A*, 2017, **5** (17), 7811-7815.

6 C. H. Kuan, S. N. Afraj, Y. L. Huang, A. Velusamy, C. L. Liu, T. Y. Su, X. Jiang, J. M. Lin, M. C. Chen and E. W. G. Diau, *Angewandte Chemie*, 2024, e202407228.

7 Q. Liao, Y. Wang, M. Hao, B. Li, K. Yang, X. Ji, Z. Wang, K. Wang, W. Chi and X. Guo, *ACS Applied Materials*, 2022, **14** (38), 43547-43557.

8 S. Zhang, R. Wu, C. Mu, Y. Wang, L. Han, Y. Wu and W. H. Zhu, *ACS Materials* Letters, 2022, **4** (10), 1976-1983.

9 S. N. Afraj, C. H. Kuan, J. S. Lin, J. S. Ni, A. Velusamy, M. C. Chen and E. W. G. Diau, *Advanced Functional Materials*, 2023, **33** (17), 2213939.

10 F. Matteocci, L. Cinà, E. Lamanna, S. Cacovich, G. Divitini, P. A. Midgley, C. Ducati and A. Di Carlo, *J Nano Energy*, 2016, **30**, 162-172.

11 S. G. Kim, T. H. Le, T. de Monfreid, F. Goubard, T. T. Bui and N. G. Park, *J Advanced Materials*, 2021, **33** (12), 2007431.

12 Z. Yao, F. Zhang, L. He, X. Bi, Y. Guo, Y. Guo, L. Wang, X. Wan, Y. Chen and L. Sun, *J Angewandte Chemie*, 2022, **134** (24), e202201847.

13 Z. Yao, F. Zhang, Y. Guo, H. Wu, L. He, Z. Liu, B. Cai, Y. Guo, C. J. Brett and Y. Li, *J Journal of the American Chemical Society*, 2020, **142** (41), 17681-17692.

14 Z. Zhu, D. Zhao, C. C. Chueh, X. Shi, Z. Li and A. K. Y. Jen, *J Joule*, 2018, **2** (1), 168-183.

15 X. Ji, T. Zhou, Q. Fu, W. Wang, Z. Wu, M. Zhang, X. Guo, D. Liu, H. Y. Woo and Y. Liu, *J Advanced Energy Materials*, 2023, **13** (11), 2203756.

16 S. You, F. T. Eickemeyer, J. Gao, J. H. Yum, X. Zheng, D. Ren, M. Xia, R. Guo, Y. Rong and S. M. Zakeeruddin, *J Nature Energy*, 2023, **8** (5), 515-525.

17 Z. Chang, J. Guo, Q. Fu, T. Wang, R. Wang and Y. Liu, *J Solar RRL*, 2021, **5** (5), 2100184.

18 J. Zhang, Q. Sun, Q. Chen, Y. Wang, Y. Zhou, B. Song, X. Jia, Y. Zhu, S. Zhang and N. Yuan, *J Solar Rrl*, 2020**, 4** (3), 1900421.

19 Y. Wang, Q. Chen, J. Fu, Z. Liu, Z. Sun, S. Zhang, Y. Zhu, X. Jia, J. Zhang and N. Yuan, *J Chemical Engineering Journal*, 2022**, 433**, 133265.

20 Y.K. Wang, H. Ma, Q. Chen, Q. Sun, Z. Liu, Z. Sun, X. Jia, Y. Zhu, S. Zhang and J. Zhang, *J ACS Applied Materials*, 2021, **13** (6), 7705-7713.